

1 **Computing Urban blue green space and its impact on urban heat island**
2 **and ecological index using multi sensor data at planned city Gandhinagar,**
3 **Gujarat, India**

4 **Tanushree Gupta¹, Rina Kumari^{1*}**

5 ¹ School of Environment and Sustainable Development, Central University of Gujarat,
6 Gandhinagar, India

7 Corresponding Author- rina.sesd@cug.ac.in; kmreenaraj@gmail.com

8
9
10
11
12
13
14
15
16
17
18
19
20
21
22
23
24
25
26
27
28
29
30

31 **Abstract**

32 *Cities are experiencing considerable changes in regional landscape patterns and ecological structure. Hence, it*
33 *is crucial to comprehend the spatial linkages between landscape patterns and ecological networks for optimal*
34 *functioning of urban ecosystems. Urban heat island (UHI) is one of the most important sensitive parameters to*
35 *understand the ecological vulnerability of cities. Gandhinagar, the green city of Gujarat, is showing a huge*
36 *landscape transformation which has been assessed by remote sensing ecological index (RSEI) with multi-*
37 *spectral satellite data for the year 2006, 2018 and 2022. We used the cellular automata land use simulation*
38 *model to predict the landscape changes and Landsat data for ecological sensitivity to correlate the urban heat*
39 *island effects in the city. The result shows an increase in 100% urban sprawl in the district since 2006 which led*
40 *to surface urban heat island (SUHI) effect. The Land Use Land Cover change dynamics shows that 100 km² of*
41 *agriculture land has been converted to built-up and wasteland. The accelerated change has been predicted with*
42 *Artificial Neural Network model with MOLUSCE tool in QGIS. The results show further decreasing trend of*
43 *agriculture land to be converted to commercial buildings and other classes. The ecological sensitivity of the*
44 *green city has been calculated with four vital indices which are wetness, dryness, greenness, and heat index.*
45 *Principal component analysis (PCA) is used to automatically assign the rank and weight of individual*
46 *parameters based on their importance in index development. The PCA reveals that the ecological index RSEI of*
47 *2006 was better than 2018 and further improved in 2022 after the country shutdown in post covid.*

48 **Keywords:** *Green city, Ecological sensitivity, SUHI, MOLUSCE (Modules for Land Change Evaluation),*
49 *Cellular Automata, Remote Sensing Ecological Index*

50 **1. Introduction**

51 The world is currently experiencing widespread urban sprawl of about 168% between 2001 to
52 2018 with highest at Asia and Africa which is a key problem for sustainable development
53 (Dewan et al. 2021; Ackerschott et al. 2023). These induced changes has vast implications on
54 natural surfaces resulting in multiple environmental effects interwoven with sustainable
55 development which are noticeable with local climate and biodiversity loss (Kong et al. 2019;
56 Dewan et al. 2021). Consequently, land use is linked with Sustainable Development Goals of
57 United Nation, particularly SDG-15 which is “Life on Land”. The goal demands to “protect
58 restore and promote sustainable use of terrestrial ecosystems, sustainably manage forests,
59 combat desertification, and halt and reverse land degradation”. In addition to the UN's

60 defined international goals for land use, several nations have set particular targets as part of
61 their sustainable development policies due to the significance of land use for sustainable
62 development. There are a number of spatial planning-related strategies that could be used,
63 including centralized systems, zoning, strategic planning, and land use allocations (Schmidt
64 2009; Jost et al. 2021). However, the international and national sustainability goals for land
65 use are currently off course.

66 Urban population have become the key driver of changing global ecosystems by increasing
67 anthropogenic impervious areas (Gong et al. 2020). Urbanization has led to landscape
68 changes, degrades environmental livelihood (Hondula et al. 2014), pollute the ambient air
69 and water quality (Adeyeri et al. 2017). Such conversions of natural lands cover to artificial
70 impervious surfaces primarily asphalt and concrete leads to development of UHI
71 phenomenon due to increase in land surface temperature (Ahmed et al. 2023). UHI is the
72 most obvious effect of urbanization and a blatant indicator of environmental degradation
73 which can be defined as the temperature difference between urban and rural surroundings as a
74 result of human activity. Although human activities are the primary drivers of the UHI
75 phenomena, other natural elements, such as geographic location like coastal, hilly or desert
76 areas, seasonal variation as summer, monsoon and winter, climate type like semiarid, arid and
77 humid, and topographical conditions, also have an impact. Additionally, the local weather
78 conditions have an impact on the air temperature like cooling influence in coastal locations
79 and heat waves in tropical and semi-arid regions (Zhou et al. 2020). Urban heat island effect
80 is one of the most well-known effects of urbanization on local climate which exacerbate the
81 energy consumption of the cities for cooling demands.

82 The land use simulation model is an efficient tool to forecast changes in land use and its
83 consequences on increased temperature with thermal infrared remote sensing data (Purswani
84 et al. 2022). The model simulation uses pre-requisite steps to identify drivers of land use
85 change which include distance from urban center, roads, waterbodies, and elevation etc. With
86 advancement of geomatics and resolution of remote sensing datasets, a number of land use
87 simulation models are available which has been studied in detail by various authors
88 (Chughtai et al. 2021; Gomes et al. 2021). These models are applicable in predicting rural
89 development and urban growth with special attention to conservation areas and dynamics of
90 shifting cultivation. Models help in urban planning, establishment of infrastructure, meeting

91 transportation and utility demand, and the identification of risky zones. The techniques are
92 also available for complex landscape settings and appropriate models for various earth's land
93 surface like vegetation, urbanization, delta region, mountainous region, coastal zone,
94 desertification, and watershed (Chughtai et al. 2021). Cheng et al used DINAMICA model to
95 simulate the changes in Amazonian colonization border (Cheng et al. 2020). Cellular
96 automata SLEUTH model was constructed to project global urban growth probability from
97 2020 to 2050 (Zhou et al. 2019). The remote sensing and GIS tools have cooperatively made
98 the prediction easy to monitor from past to present and future. Many artificial neural
99 networks have been found to be efficient to work with, for example, MLP-ANN based model
100 with cellular automata simulation like MOLUSCE plugin. MOLUSCE tool was found to be
101 popularly known for its flexible and accurate mapping.

102 The plugin includes several well-known algorithms, such as cross-tabulation methods, utility
103 modules, and algorithmic modules, such as multi-criteria evaluation (MCE), weights of
104 evidence (WoE), logistic regression (LR), and Monte Carlo cellular automata (CA) models
105 (Muhammad et al. 2022). The MOLUSCE tool in QGIS is freely accessible and easily
106 monitored which has been used for land use prediction and change detection study for the
107 year 2030 in this study.

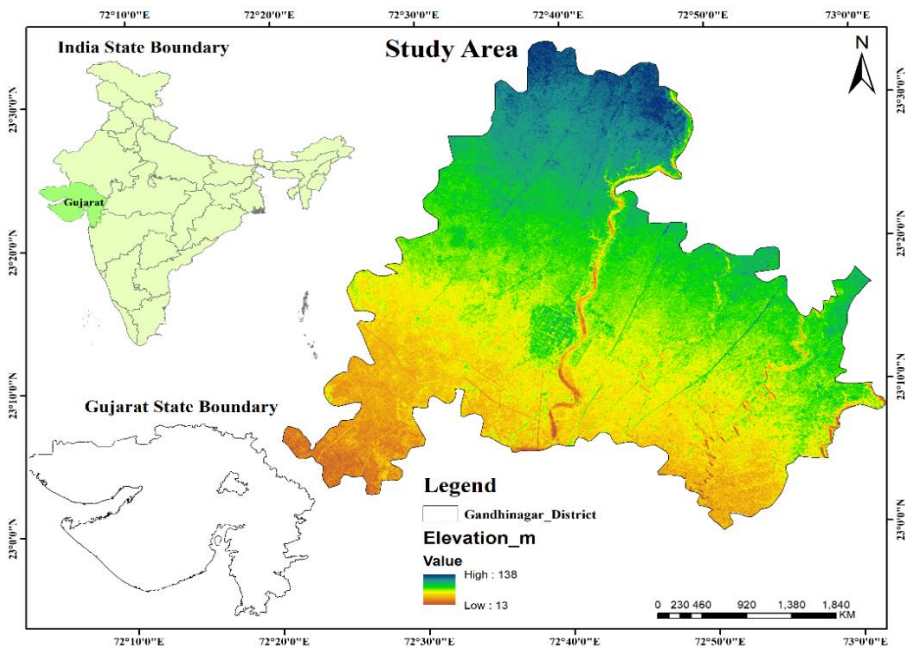
108 The study has been carried out in the tree capital of India, Gandhinagar which is the second
109 planned city of India after Chandigarh and first smart city after GIFT city hub. Being in the
110 close proximity to Ahmedabad, the city has expanded which has influenced the ability to
111 sustain its ecosystem services. Thus, the aim of this study is to investigate the trend of change
112 in land use with reference to already published study at Gandhinagar district its impact on
113 LST causing surface heat island effect that might influence the ecological quality of the study
114 area.

115 **2. Datasets and Methods**

116 **2.1 Description of the Study Area**

117 The current research is performed at smart city Gandhinagar situated between Lat 22°56' and 23°36' and
118 Long 72°23' to 73°05' (fig. 1). The district has four talukas with nine urban centers and 291 villages. The
119 study region features a perennial river system and a semi-arid environment, which makes it dry for most of
120 the year. The rainfall occurs in June to September, of which 95% is received from the southwest. According

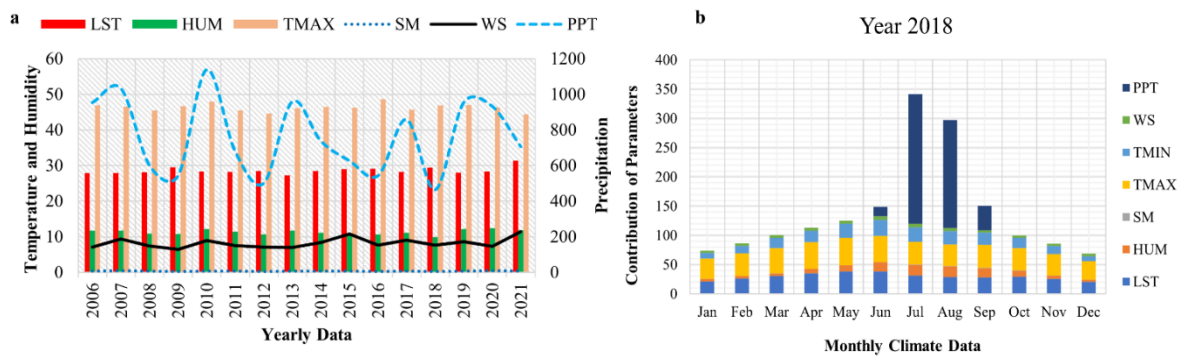
121 to IMD gridded data, the actual rainfall is 824mm during Jan to dec 2022 with 8% deviation from normal
 122 rainfall (Wris.gov.in). The maximum temperature during summer reaches up to 41°C and sometimes
 123 affected by cold wave from western disturbances (Central Ground Water Board 2014). The relative
 124 humidity reaches 65% in monsoon and drops to 20% or less in the driest months (fig. 2). The population
 125 growth rate has been increasing to 12.5 % every decade since 2001 due to close proximity to Ahmedabad
 126 city. The district covers approximately 2137 km² which is 1.09% of Gujarat state with population of
 127 1,934,537 as counted in December 2023 (uidai.gov.in). For accommodation of such huge population
 128 transformation, the city is expanding at the north and south direction mostly in the peripheral region
 129 towards Ahmedabad.



130

131

Fig. 1 Study area description and RGB images of district Gandhinagar



132

133 **Fig. 2** Temporal Climate Data at Gandhinagar station and monthly contribution of individual parameters (LST-
 134 land surface temperature, HUM- humidity, Tmax- air temperature max, Tmin- air temperature min, SM- soil
 135 moisture, WS- Wind speed, PPT- precipitation)

136 **a. Data**

137 This study utilizes Landsat-TM, OLI, LISS-IV and climate data products for spatio-temporal
 138 monitoring of environment from 2006 to 2022 (Table 1). Landsat data level-2 products were
 139 obtained, then adjusted atmospheric and radiometric correction along with scan line error
 140 correction in Landsat-7. In order to get the consistent data, images are compared from both
 141 the years by uniformly selecting the May month at minimum cloud cover. The images are
 142 further layer stacked and clipped according to study area after pre-processing and respective
 143 indices were calculated afterwards. The land use classification is done using onscreen manual
 144 digitization with LISS-IV imageries. The LISS-IV dataset is provided by the National
 145 Remote Sensing Center (nrsc.gov.in), which has been comprehensively evaluated with first
 146 level of classification system at 90% accuracy status. Further dynamic modelling of land
 147 cover was performed in MOLUSCE tool of QGIS software based on multi-layer perceptron
 148 (MLP) neural network showing 0.59 kappa coefficient with 1000 iteration. The methodology
 149 of data processing and datasets used at their respective GIS software are further explained in
 150 fig. 3.

151 **Table 1.** Information of remote sensing data acquired at different time interval

Year	Data type	Date	Path/Row	Cloudiness
2006	Landsat TM	2006-05-16, 2006-05-06	148/44, 149/44	Less than 10%
2018, 2022	Landsat OLI	2018-05-25, 2018-05-16 2022-05-11, 2022-05-20	148/44, 149/44 148/44, 149/44	Less than 10%
2006	LISS-IV	2006-05-16, 2006-05-06	93/55-56	NA
2018	LISS-IV	2018-05-25, 2018-05-16	93/55-56	NA

152

153 **2.3 Land use classification and accuracy assessment**

154 Cloud free Resourcesat-2 LISS-IV images of the study area are acquired by NRSC at the Space Application
 155 Centre Ahmedabad at the dry season to avoid the seasonal fluctuation in LULC (Johansen et al. 2015). To
 156 enhance the quality of images, the data was pre-processed in ENVI 5.2 utilizing geometric, atmospheric, and
 157 radiometric correction. Before classification all the bands were layer stacked, mosaicked and subset in ERDAS
 158 IMAGIN software. The entire study area was classified using Onscreen digitization into four classes as
 159 Agriculture land, waterbody, Wasteland, and Built-up. The accuracy assessment is done using random point
 160 generation and validated in Google Earth showing 90% total accuracy which supports the results of true values
 161 with google earth data. For the overall accuracy percentage of matched number of sites to the total no. of sites
 162 has been calculated with the formula given below. The accuracy of individual land use classes is also calculated
 163 in the same manner.

164
$$\text{Overall accuracy} = \frac{\text{Total number of correctly classified points}}{\text{total number of reference points}} * 100 \text{ Eq. 1}$$

165 **2.4 Calculation of remote sensing ecological index (RSEI)**

166 The RSEI was first developed in 2013 to track the eco-environmental quality using the primary variables of
 167 greenness, wetness, dryness, and heat. The purpose of RSEI is to accomplish the convenient and fast results to
 168 visualize ecological environment. It can provide valuable information about the health status of ecosystem. The
 169 index has been utilized to observe the ecosystem of cities and monitor the urban environment which is
 170 calculated with equation 2.

171
$$RSEI = PCA(NDVI, TCW, NDBSI, LST) \text{ Eq. 2}$$

172 **2.4.1 Green Index-** Vegetation is an important part of terrestrial ecosystem which plays a significant role in
 173 various climatic phenomenon. Normalized Difference Vegetation Index can be calculated using NIR and RED
 174 bands of Landsat data which clearly indicates the vegetation coverage and nutritional information (Gao et al.
 175 2022). The values generally range between -1 to +1, indicating poor and rich vegetation respectively.

176
$$NDVI = \frac{NIR-RED}{NIR+RED} \text{ Eq. 3}$$

177 **2.4.2 Humidity/Wetness Index-** The tasseled cap represents the environmental changes which describe the
 178 water and soil moisture. Wetness is represented by wet component of tasseled hat transformation which can be

179 calculated by equation 4 and 5 (Crist 1985). The wetness index gives information of water content of soil and
 180 vegetation where constants vary according to dataset utilized.

$$181 \quad WIETM = 0.0315\rho_{blue} + 0.2021\rho_{green} + 0.3012\rho_{red} + 0.1594\rho_{nir} - 0.6806\rho_{swir1} -$$

$$182 \quad 0.6109\rho_{swir2} \text{ Eq. 4}$$

$$183 \quad WIOLI = 0.1511\rho_{blue} + 0.1973\rho_{green} + 0.3283\rho_{red} + 0.3407\rho_{nir} - 0.7117\rho_{swir1} - 0.4559\rho_{swir2}$$

$$184 \quad \text{Eq. 5}$$

185 Where multiplication values are the coefficients and obtained from tasseled hat transformation of wetness index
 186 of Landsat TM and OLI with the literature (Crist 1985). ρ_{blue} , ρ_{green} ,... are the bands of Landsat data.

187 **2.4.3 Dryness Index-** The ecological pattern of urban ecosystems is greatly influenced by LULC change within
 188 and beyond their boundaries. Among them, the change of ecological land to construction purpose is the notable
 189 physical feature, therefore build-up and soil index are used to represent the anthropogenic forces on
 190 environment. This index is characterized by built-up index (NDBI) and bare soil index (BSI). It represents no
 191 vegetation or negligible soil moisture which is due to replacement of natural land surface to built-up and bare
 192 soil. The expression of these indices are given in eq 6-8.

$$193 \quad NDBI = \frac{SWIR - NIR}{SWIR + NIR} \text{ Eq. 6}$$

$$194 \quad BSI = \frac{(SWIR+NIR)-(NIR+BLUE)}{(SWIR-NIR)+(NIR+BLUE)} \text{ Eq. 7}$$

$$195 \quad NDBSI = \frac{NDBI+BSI}{2} \text{ Eq. 8}$$

196 **2.4.4 Heat Index/LST-** Urbanization alters the surface energy balance of urban ecosystem as compared to
 197 surrounding rural areas. Temperature not only affects the evolution of organisms, but also slight changes might
 198 be harmful to their development. In the following study heat index is calculated in terms of LST using band 10
 199 in Landsat-OLI and band 6 in Landsat TM. The steps of LST calculation are differentiated into three sections:
 200 the conversion of atmospheric radiation brightness, the radiation brightness of ground through the atmosphere to
 201 satellite sensor, and energy reflected towards the ground as employed by various authors (Malik and Shukla
 202 2018; Liu et al. 2021; Dutta et al. 2021). This study uses the LST calculation as done by Sukanya et al. 2022.

203 **2.5 Standardization of indices and combination of indicators**

204 Based on the above equation for various indices, we aimed to design the ecological index which allows the
205 quick assessment of ecosystem quality. The quantitative interval of these four indices is different which are
206 standardized by reclassification to get the values between 0 to 1 (eq. 14) (Carlson and Arthur 2000). The
207 standardized images are run in PCA to get compressed multi-dimensional data with the relative importance of
208 individual parameters and avoid impact of co-linearity between variables (Seddon et al. 2016). The weight or
209 individual parameters are automatically assigned according to their contribution and prevent error in assigning
210 weights in individual characteristics. ArcGIS PCA in spatial analyst tool is used to combine data into four
211 bands PCA which is further calculated with eq. 15 to derive the final RSEI which falls between 0 to 1, the close
212 values of RSEI to 1 entails the better ecological sustainability. The percentage eigen values and contribution of
213 individual parameters is explained in table 3.

214
$$NDVIstd = \left(\frac{NDVI - NDVImin}{NDVImax - NDVImin} \right) Eq. 14$$

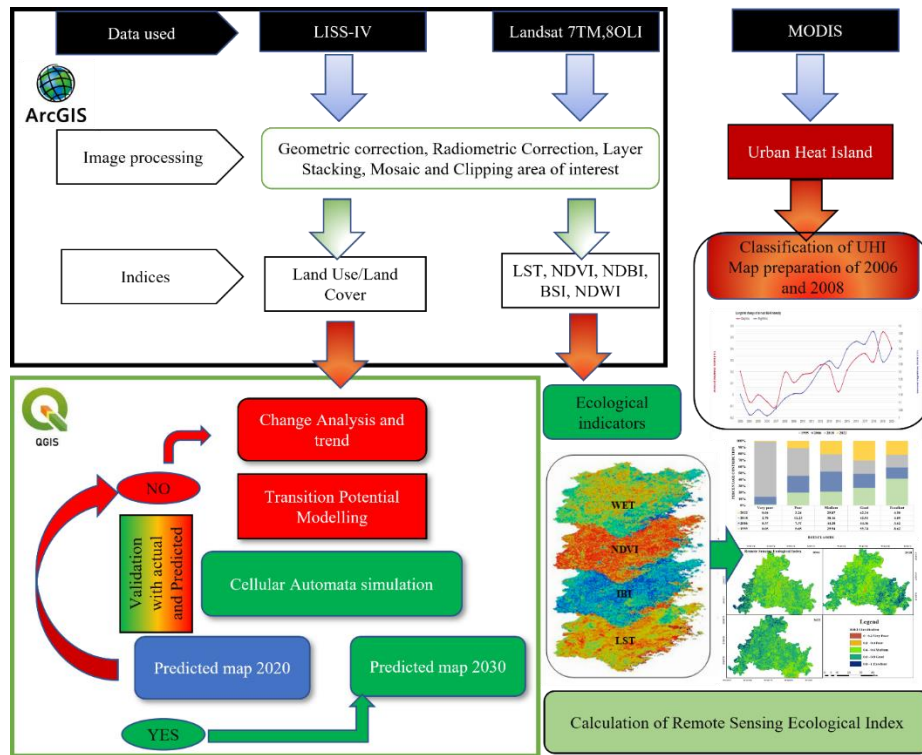
215
$$RSEI = \left(\frac{PCA - PC Amin}{PC Amax - PC Amin} \right) Eq. 15$$

216 **2.6. Principal Component Analysis (PCA)**

217 PCA explains the variability and reduces the dimensions of multiple datasets into a index values. It performs on
218 a set of raster bands to give a single multiband raster output. Here the percentage variance identifies the amount
219 of variance each eigenvalues captures which is useful to interpret the results of PCA. If very few eigenvalues are
220 capturing the majority of variance, it is adequate to use this subset of bands in the analysis since they represent
221 the majority of interaction within the dataset. The components having greater than 1 value are taken into
222 consideration to understand the dominant parameter [Seddon et al. 2016, Campbell and Wynne 2011].

223 **2.7 Surface Urban Heat Island effect**

224 SUHI calculation was done as discussed in Sukanya et al, 2022. Two urban centers are identified in the study
225 area, the city center Gandhinagar and Kalol taluka for comparison of the study.



226

 227 **Fig. 3** Flow chart of selected dataset, applied Methodology and GIS platform to analyze the

228

data

 229 **3 Results and Discussion**

 230 **3.1 Change in LULC between 2006 to 2018 and projected expansion**

231 The time series analysis of land cover change map has been presented (fig. 4-5). LULC statistics and transition

232 patterns help to relate the forces behind the shifting of land use. The district has been classified under four major

233 land use categories present in the study area which are Agriculture land, waterbody, built-up, and shrub

 234 land/wasteland. The most drastic change has occurred in built-up area which has expanded from 110 km² of

 235 land covered with residential and industrial area in 2006 to 181 km² in 2018. The maximum area was

236 contributed by agriculture and bare land. The sides of the roads and construction of new roads are contributed by

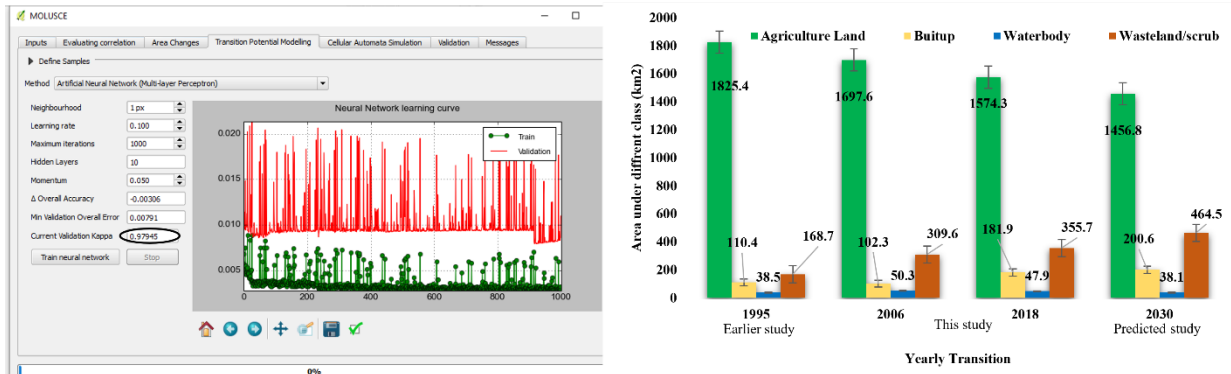
 237 small scrubs. The river systems have been improved since 1995 as total area was occupied by only 38.4 km² of

 238 the area which has improved to 50 km². The extension of canal system at the north of the district has contributed

239 to the increased water structure while at the same time small waterbodies disappeared due to increasing

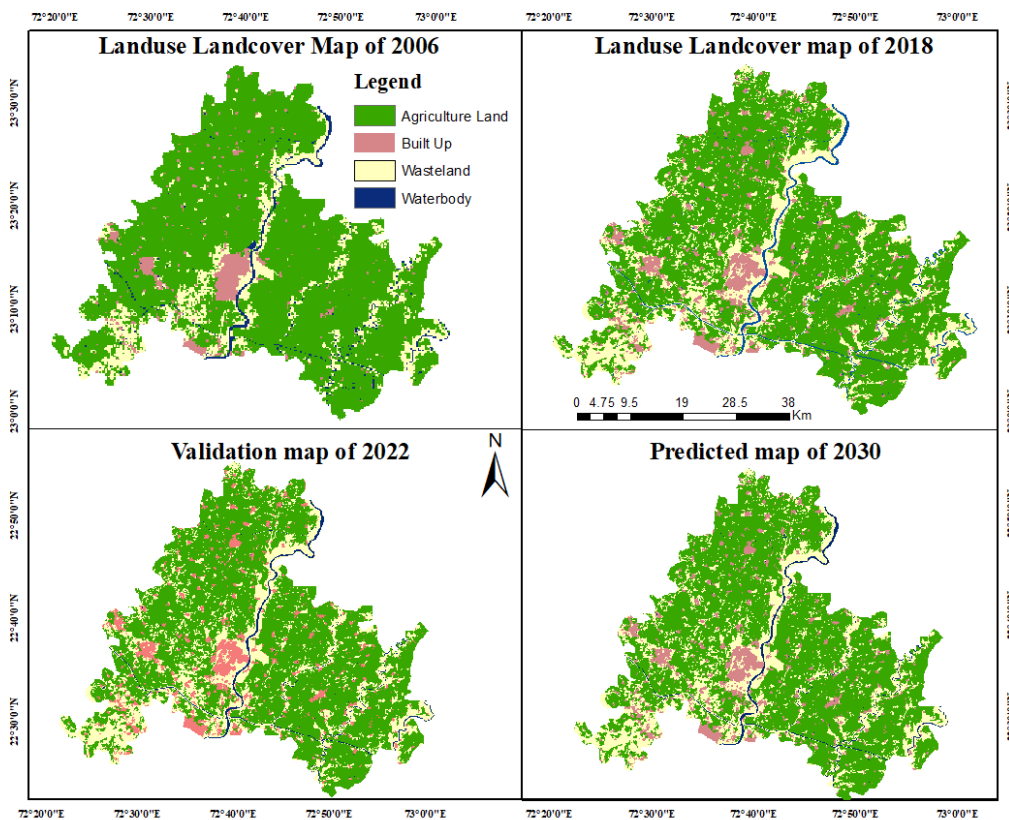
 240 anthropogenic pressure. Hence after 2018, the waterbodies further decreased to 47.9 km² and predicted to

241 decrease by 38.1 km² in 2030. The wasteland comprises 168 km² in 1995, while in 2006 it has increased to
 242 294.6 km² and this area is continuously increasing to 350 km² and further the prediction map shows 484 km² in
 243 2030. Agriculture, being the dominant class, has declined drastically from 1825 km² to 1456 km² till 2030 (fig.
 244 4).



245

246 **Fig. 4** Transition potential in MOLUSCE model and temporal variation of change in land use from 1995 to 2030

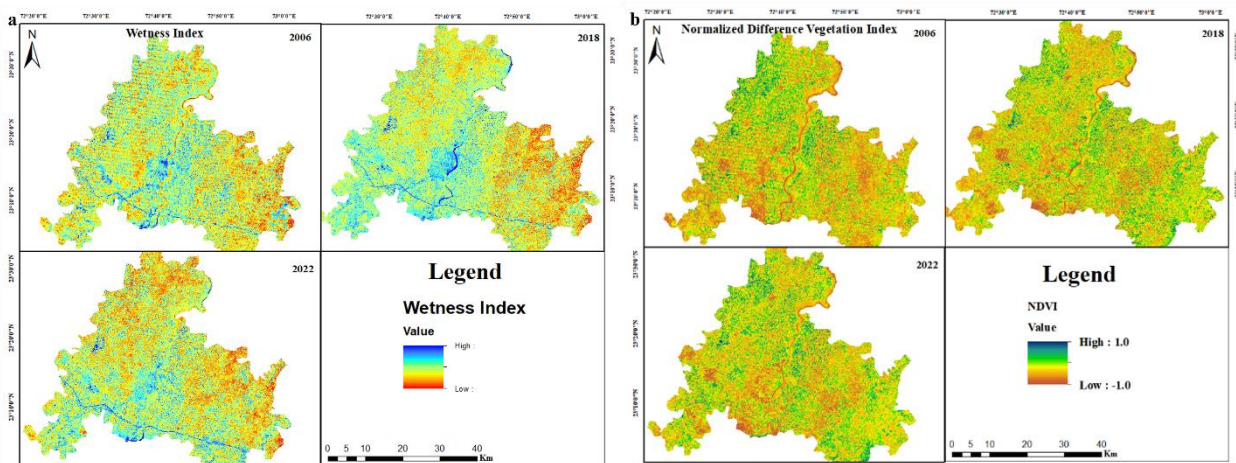


247

248 **Fig. 5** Land use Land cover maps of two consecutive years with validation and prediction

249 3.2 Biophysical parameters of the study area

250 In this study we have computed vegetation in terms of NDVI, wetness as NDWI, dryness index as NDBSI and
 251 heat as LST as given in table 4. Fig. 6a explains the spatial variation of wetness index which is an important
 252 factor in RSEI because it helps in growth and productivity of ecosystem as plants require water to thrive. The
 253 index shows that there is a drastic decline was found in surface wetness after 2006 while a slight moisture has
 254 increased till 2022. The results are consistent with greenness index of area which falls between -0.24 to 0.77 in
 255 2006 and -0.06 to 0.66 in 2018 with further increment till 2022 (fig. 6b). The positive values remark healthy
 256 vegetation and negative values are reflected by bare impervious land. The maximum value of NDVI is found to
 257 be 0.96 in 2022 due to limited destruction of natural resources after the covid lockdown. The overall results
 258 significantly explain that vegetation quality has declined due to changing natural landscape till now. On the
 259 other hand, the spatial variation of dryness index, which is the combination of built-up and soil index, also
 260 varies accordingly (fig. 7a). The values have increased from 0.61 to 0.7 and 0.8 till 2022 because of the
 261 declining vegetation and wetness of the area. Overall, these indices play a crucial role in obtaining the
 262 ecosystem quality of the study area.



263

264

Fig. 6 Spatial maps of biophysical parameters a) Wetness index and b) Greenness Index

265

266

267

Table. 2 Statistics of minimum maximum mean of four indices used for ecological index

Parameters/Years	Min			Max			Mean			St Dv		
	2006	2018	2022	2006	2018	2022	2006	2018	2022	2006	2018	2022
Green Index	-0.24	-0.06	-0.15	0.77	0.66	0.96	0.26	0.26	0.29	0.09	0.07	0.08
Wet Index	-0.55	-0.41	-0.46	0.23	0.06	0.09	-0.2	-0.13	-0.1	0.04	0.03	0.04
Dry Index	-1.09	-0.64	-1.67	0.61	0.7	0.83	0.1	0.09	-0.26	0.15	0.09	0.19
Heat Index	20.26	30.7	30.15	50.79	49.6	48.67	38.07	41.19	42.04	3.17	1.93	2.98

268

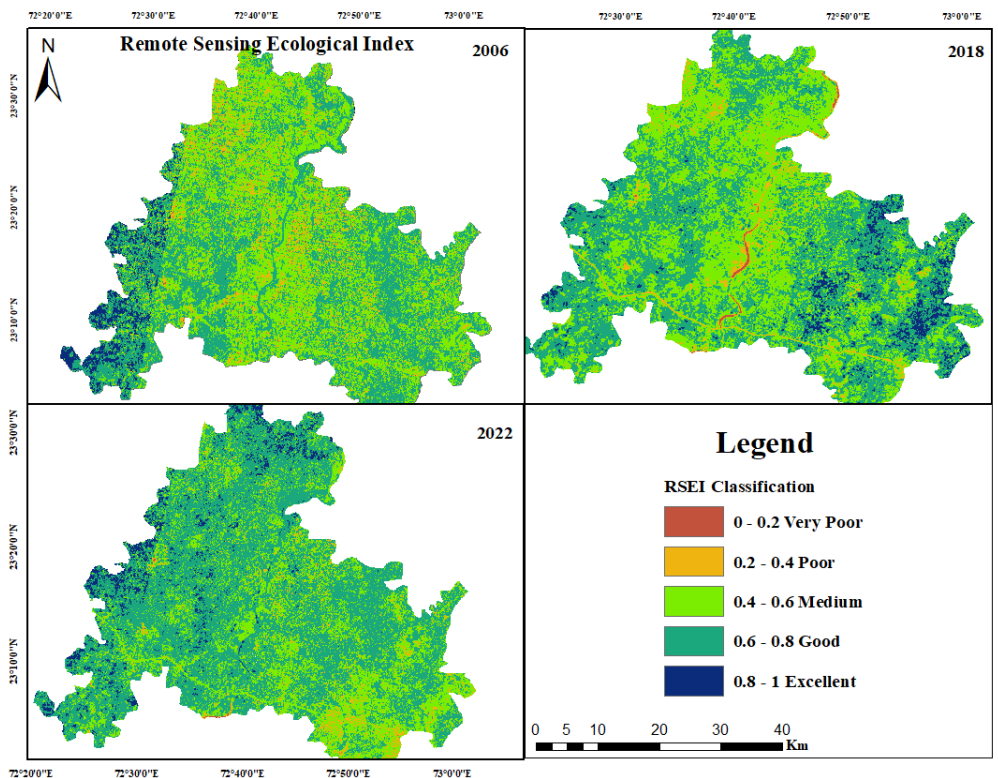
269 3.6 Ecological sensitivity of the study area

270 In order to study the contribution of individual parameters (wetness, greenness, dryness and heat index) on RSEI
 271 values, Principal Component Analysis is done using ArcGIS 10.3. In table 2 the statistical data of individual
 272 components with their eigen values are given to understand the contribution of individual parameters on
 273 assessment of ecosystem quality. The factors which promote the quality of ecosystem were found to be
 274 degraded while unfavorable parameters like dryness and LST have increased to almost 50% in high and very
 275 high category (fig. 7). The greenness index has shrunk from 0.77 to 0.66 likewise the moisture content in the
 276 area was found slightly high at the central part where the river and canals are passing. The negatively affecting
 277 parameters, which are dryness and heat index, both have increased from 2006 to 2018 and further improved in
 278 2022.

279 On the basis of these characteristics the remote sensing based ecological index has been developed. The
 280 descriptive analysis of the index shows that the ecosystem has been degraded since the area under poor RSEI
 281 values has drastically increased from 2006 to 2018 (fig. 12). At the same time the ecosystem has also improved
 282 due to the covid lockdown which has reflected at better ecosystem index in 2022. The values ranged between
 283 0.0 to 1.05 and 0.0 to 1.21 during 2006 and 2018 respectively. Although the maximum values had increased
 284 from 1.05 to 1.21 with mean of 0.61 to 0.72 between 2006 to 2018 respectively but overall, the spatial extent has
 285 reduced. The effect of lockdown is also visible as improved ecosystem quality (RSEI_{mean}=0.88) was noticed in
 286 2022. Few studies have also reported that natural resources were found to be rejuvenated at this time in Indian
 287 cities (Mishra et al. 2021; Joshi et al. 2022).

288 According to the technical criteria for good ecosystem quality, RSEI is divided into five classes that says <0.2
 289 are very poor, 0.2-0.4 poor, 0.4-0.6 medium, 0.6-0.8 good and 0.8 to 1.0 are excellent (Gao et al. 2022). The

290 spatial distribution map of RSEI shows that the central part of the study where all the major cities and villages
 291 are present have very poor ecological quality during both the study period. The area falling under very poor
 292 class increased from 7.8 km² to 58.3 km² which is due to increased built-up area. Likewise, the poor categories
 293 have also gained the area from 7.3 to 12.2%. The study area has undergone the construction of GIFT (Gujarat
 294 International Finance Tech) city and metro which has destroyed a vast natural resource and contributed to
 295 destruction of vegetation and wetness earlier in the area. The ecosystem has also improved due to plantation in
 296 the city as reported by GEER foundation, the RSEI values in Excellent class has gained almost 10 km² of area
 297 under this category proving the richness of vegetation due to tree plantation.



298

299 **Fig. 7.** Spatial Variation of Remote Sensing Ecological Index

300 **5.0 Conclusion**

301 This study examines the land cover changes in green city Gandhinagar that demonstrate a significant urban
 302 sprawl since the previous study carried out in the area. The primary changes in the land cover between 2006 and
 303 2018 were decrease in agricultural land and an increase in built-up area. This behavior was mostly noticed at the
 304 southern area adjacent to Ahmedabad district and urban extension in Gandhinagar city. The land cover

305 prediction based on CA-MLP showed satisfactory results for the district as kappa coefficient and percentage
306 accuracy was 0.60 and 78% accuracy after 1000 iterations. The predicted map shows decreasing agriculture with
307 minute changes in urban class while wasteland was increasing according to the prediction model till 2030. The
308 result of increasing impervious surface is affecting LST which give rise to urban heat island effect. There is a
309 significant increasing trend of LST of 2°C during the summer season from 2006 to 2018 which is influencing the
310 UHI of the district. The annual daytime and nighttime SUHI intensity of the district was found to be increased
311 from 0.2 to 0.4 and 0 to 1.45 from 2003 to 2020 respectively which might influence the ecosystem of the urban
312 dwellers. Further, till 2022 the improved surface temperature was noticed with improved biophysical factors like
313 vegetation and wetness in the study area as an effect of post covid lockdown. The quality of urban ecosystem is
314 identified using remote sensing ecological index by integrating four related indices important to human survival
315 which are vegetation, wetness, dryness and heat index. The individual contribution of indices is noticed with
316 principal component analysis. The vegetation richness was found to be degraded by 2018 as the classification
317 shows that 44.2 km² of the area comes under rich vegetation while it was 84 km² during 2006. Likewise, the
318 ecosystem quality was found to be decreased in medium and good quality classification while poor and very
319 poor class has increased which clarifies that overall quality of ecosystem has degraded. This study shows that
320 urban development has certain interferences on ecological environment therefore it is important to integrate
321 ecological research to protect the sustainability of urban ecosystem. Hence effective urban green infrastructure
322 planning and management are vital for creating sustainable, resilient, and inclusive cities to fulfill the
323 Sustainable Development Goals by 2030.

324 **Data Availability**

325 All the data analyzed during the study are included in this research article.

326 **Acknowledgement**

327 The authors are thankful to the NRSC for providing the data & SERB for providing the fund
328 (ECR/000202/2016).

329 **Few References**

330 Ackerschott A, Kohlhase E, Vollmer A, et al (2023) Land Use Policy Steering of land use in the context of
331 sustainable development : A systematic review of economic instruments. 129:.

- 332 <https://doi.org/10.1016/j.landusepol.2023.106620>
- 333 Adeyeri OE, Akinsanola AA, Ishola KA (2017) Investigating surface urban heat island characteristics over
334 Abuja, Nigeria: Relationship between land surface temperature and multiple vegetation indices. *Remote*
335 *Sens Appl Soc Environ* 7:57–68. <https://doi.org/10.1016/j.rsase.2017.06.005>
- 336 Afrakhteh R, Asgarian A, Sakieh Y, Soffianian A (2016) Evaluating the strategy of integrated urban-rural
337 planning system and analyzing its effects on land surface temperature in a rapidly developing region.
338 *Habitat Int* 56:147–156. <https://doi.org/10.1016/j.habitatint.2016.05.009>
- 339 Ahmed S, Bindajam A, Waseem M, et al (2023) Response of soil moisture and vegetation conditions in seasonal
340 variation of land surface temperature and surface urban heat island intensity in sub - tropical semi - arid
341 cities. *Theor Appl Climatol* 367–395. <https://doi.org/10.1007/s00704-023-04477-2>
- 342 Ariken M, Zhang F, Liu K, et al (2020) Coupling coordination analysis of urbanization and eco-environment in
343 Yanqi Basin based on multi-source remote sensing data. *Ecol Indic* 114:106331.
344 <https://doi.org/10.1016/j.ecolind.2020.106331>
- 345 Bento VA, Gouveia CM, DaCamara CC, et al (2020) The roles of NDVI and Land Surface Temperature when
346 using the Vegetation Health Index over dry regions. *Glob Planet Change* 190:103198.
347 <https://doi.org/10.1016/j.gloplacha.2020.103198>
- 348 Budhiraja B, Agrawal G, Pathak P (2020) Urban heat island effect of a polynuclear megacity Delhi –
349 Compactness and thermal evaluation of four sub-cities. *Urban Clim* 32:100634.
350 <https://doi.org/10.1016/j.uclim.2020.100634>
- 351 Campbell, J.B. and Wynne RH (2011) *Introduction to Remote Sensing*. Guilford Press
- 352 Carlson TN, Traci Arthur S (2000) The impact of land use - Land cover changes due to urbanization on surface
353 microclimate and hydrology: A satellite perspective. *Glob Planet Change* 25:49–65.
354 [https://doi.org/10.1016/S0921-8181\(00\)00021-7](https://doi.org/10.1016/S0921-8181(00)00021-7)
- 355 Central Ground Water Board (2014) *Ground Water Brochure Gandhinagar District*. 1–33
- 356 Cheng L lin, Liu M, Zhan J qi (2020) Land use scenario simulation of mountainous districts based on Dinamica

- 357 EGO model. *J Mt Sci* 17:289–303. <https://doi.org/10.1007/s11629-019-5491-y>
- 358 Chughtai AH, Abbasi H, Karas IR (2021) A review on change detection method and accuracy assessment for
359 land use land cover. *Remote Sens Appl Soc Environ* 22:100482.
360 <https://doi.org/10.1016/j.rsase.2021.100482>
- 361 Crist EP (1985) A TM Tasseled Cap equivalent transformation for reflectance factor data. *Remote Sens Environ*
362 17:301–306. [https://doi.org/10.1016/0034-4257\(85\)90102-6](https://doi.org/10.1016/0034-4257(85)90102-6)
- 363 Devi AB, Deka D, Aneesh TD, et al (2022) Predictive modelling of land use land cover dynamics for a tropical
364 coastal urban city in Kerala, India. *Arab J Geosci* 15:. <https://doi.org/10.1007/s12517-022-09735-7>
- 365 Dewan A, Kiselev G, Botje D, et al (2021) Surface urban heat island intensity in five major cities of
366 Bangladesh: Patterns, drivers and trends. *Sustain Cities Soc* 71:. <https://doi.org/10.1016/j.scs.2021.102926>
- 367 Dutta D, Rahman A, Paul SK, Kundu A (2021) Impervious surface growth and its inter-relationship with
368 vegetation cover and land surface temperature in peri-urban areas of Delhi. *Urban Clim* 37:.
369 <https://doi.org/10.1016/j.uclim.2021.100799>
- 370 Eckstein D, Künzel V, Schäfer L, Wings M (2020) GLOBAL CLIMATE RISK INDEX 2020 Who Suffers
371 Most from Extreme Weather Events ? Weather-Related Loss Events in 2018 and 1999 to 2018
- 372 EPA (2008) EPA’s 2008 Report on the Environment. *Environ Prot EPA/600/R-07/045F*
- 373 Fei L, Shuwen Z, Jiuchun Y, et al (2018) Effects of land use change on ecosystem services value in West Jilin
374 since the reform and opening of China. *Ecosyst Serv* 31:12–20.
375 <https://doi.org/10.1016/j.ecoser.2018.03.009>
- 376 Gao YG, Li YH, Xu HQ (2022) Assessing Ecological Quality Based on Remote Sensing Images in Wugong
377 Mountain. *Earth Sp Sci* 9:. <https://doi.org/10.1029/2021EA001918>
- 378 Ghosh S, Kumar D, Kumari R (2022a) Assessing spatiotemporal variations in land surface temperature and
379 SUHI intensity with a cloud based computational system over five major cities of India. *Sustain Cities Soc*
380 85:. <https://doi.org/10.1016/j.scs.2022.104060>
- 381 Ghosh S, Kumar D, Kumari R (2022b) Assessing spatiotemporal dynamics of land surface temperature and

382 satellite-derived indices for new town development and suburbanization planning. *Urban Gov* 2:144–156.

383 <https://doi.org/10.1016/j.ugj.2022.05.001>

384 Ghosh S, Kumar D, Kumari R (2022c) Assessing spatiotemporal dynamics of land surface temperature and

385 satellite-derived indices for new town development and suburbanization planning. *Urban Gov* 2:144–156.

386 <https://doi.org/10.1016/j.ugj.2022.05.001>.

387

388

389

390

391

392

393

394

395

396

397

398

399

400

401

402

403

404

405

406

407